Quantum response to time-dependent external fields

Miyashita, Seiji; Tanaka, Shu; Raedt, Hans De; Barbara, Bernard

Published in:
Journal of Physics: Conference Series

DOI:
10.1088/1742-6596/143/1/012005

Publication date:
2009

International Workshop on Statistical-Mechanical Informatics 2008 (IW-SMI 2008) IOP Publishing
Journal of Physics: Conference Series **143** (2009) 012005 doi:10.1088/1742-6596/143/1/012005

Quantum response to time-dependent external fields

Seiji Miyashita[1,5], Shu Tanaka[2], Hans De Raedt[3], and Bernard Barbara[4]

[1] Department of Physics, Graduate School of Science, The University of Tokyo, 7-3-1 Hongo, Bunkyo-Ku, Tokyo 113-0033, Japan
[2] Institute for Solid State Physics, The University of Tokyo, 5-1-5 Kashiwanoha, Kashiwa, 277-8581, Japan
[3] Department of Applied Physics Zernike Institute of Advanced Materials University of Groningen Nijenborgh 4, NL-9747 AG Groningen The Netherlands
[4] Laboratoire Louis Néel, CNRS 25 Ave. des martyrs, BP 166, 38 042 Grenoble Cedex 09, France.
[5] CREST, JST, 4-1-8 Honcho Kawaguchi, Saitama 332-0012, Japan

E-mail: miya@spin.phys.s.u-tokyo.ac.jp

Abstract. Recently, explicit real time dynamics has been studied in various systems. These quantum mechanical dynamics could provide new recipes in information processing. We study quantum dynamics under time dependent external fields, and explore how to control the quantum state, and also how to bring the state into a target state. Here, we investigate a pure quantum mechanical dynamics, dynamics in quantum Monte Carlo simulation and also in quantum master equation. For the control magnetic states, operators which do not commute with magnetization are important. We study case of the transverse Ising model, in which we compare natures of thermal and quantum fluctuations. We also study the cases of the Dzyaloshinsky-Moriya interaction, where we find a peculiar energy level structure. Moreover we study the case of itinerant magnetic state, where we study the change from the Mott insulator to the Nagaoka ferromagnetic state. Effects of dissipation are also discussed.

1. Introduction

Recently, quantum dynamics has attracted interest in the field of information processing, i.e., data propagation by quantum cryptography and quantum computing [1], and quantum annealing method [2]. In order to manipulate the quantum state, we need to understand how the quantum state changes under a change of external field. In general, when we study quantum dynamics, we describe a state of the system by a wavefunction which is generally a superposition of the eigenstates. Therefore, the quantum state covers all the configuration space (Hilbert space) and has an advantage in the data processing. In particular, the quantum annealing makes use of this advantage to find the desired state. Peculiar quantum properties have been found in the so-called single molecular magnets, such as Mn_{12}[3], Fe_8[4], V_{15}[5], etc. These systems could be candidates for a storage of information. Here, we will study some properties of quantum fluctuation.

2. Quantum fluctuation

2.1. single spin case

First, let us study the quantum fluctuation of a single spin system defined by

$$\mathcal{H}_{\rm TI0} = -H\sigma^z - \Gamma\sigma^x, \tag{1}$$

where σ^α denotes the α-th component of the Pauli operator

$$\sigma^x = \begin{pmatrix} 0 & 1 \\ 1 & 0 \end{pmatrix}, \quad \sigma^y = \begin{pmatrix} 0 & -i \\ i & 0 \end{pmatrix}, \quad \sigma^z = \begin{pmatrix} 1 & 0 \\ 0 & -1 \end{pmatrix}. \tag{2}$$

Here, we take the z axis as the quantization axis.

In the case $\Gamma = 0$, the magnetization of the z-component is a good quantum number and no quantum fluctuations exist. The eigenstates are given by

$$\sigma^z|+\rangle = |+\rangle, \quad \text{and} \quad \sigma^z|-\rangle = -|-\rangle. \tag{3}$$

The eigenenergies are $E_1 = -H$ and $E_2 = H$, which are depicted by the dotted lines in the Fig. 1(a) and we call them "diabatic state". When we set an initial state at a negative field (say the point denoted by the open circle in the Fig. 1(a)) and change the field to a positive large field, the state follows the curve and simply comes to the point denoted by the open triangle. Here, the spin state does not change at all.

If we add the term of Γ (the transverse field), the energy levels are given by the solid curve. In this case, the infinitesimally slow sweep of the field adiabatically leads the state to the point denoted by the closed circle. Here, the state is always in the ground state, which we call "adiabatic state". If we sweep the field with a finite speed, then some amount of the state is scattered to the excited state (the open triangle). This process is described by the Landau-Zener-Stückelberg mechanism [6, 7], where the probability of staying in the ground state is given by

$$P_{\rm LZS} = 1 - \exp\left(-\pi\frac{(\Delta E)^2}{4\hbar v \Delta M}\right), \tag{4}$$

where ΔE is the energy gap at the avoided level-crossing point ($H = 0$) and in the present case $\Delta E = 2\Gamma$, and v is the velocity of the field $dH(t)/dt$, and ΔM is the difference of the magnetizations of the diabatic state ($\Delta M = 2$). The magnetization processes $M(t)$ for various sweep speeds are depicted in Fig. 1(b)

2.2. Cooperative systems: The transverse Ising model

The effects of quantum fluctuation on the ordering phenomena have been studied. The most typical model is given by the transverse Ising model [8]

$$\mathcal{H} = -J\sum_{<ij>}\sigma_i^z\sigma_j^z - \Gamma\sum_i \sigma_i^x, \tag{5}$$

where $\langle ij\rangle$ denotes interacting pair sites. The transverse field causes tilt of spins in the classical case, and it causes spins to flip in the quantum case. Thus, this field reduces the correlation function of the z-components. In the case $\Gamma = 0$, there are two eigenstates $|++\cdots+\rangle$ and $|--\cdots-\rangle$ which are degenerate. We may consider these states as classical stable states. In the presence of Γ, the ground state is given by a linear combination of states. This state can be considered as a quantum mixing state of two classically stable states. Competition between the classical order due to the interaction $J\sum_{<ij>}\sigma_i^z\sigma_j^z$ and the quantum fluctuation due to $\Gamma\sum_i\sigma_i^x$ causes a so-called quantum phase transition in the ground state.

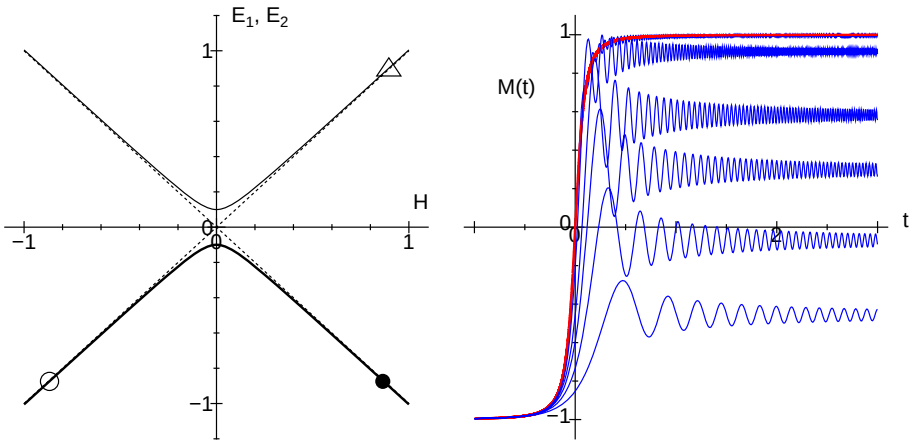

(a) (b)

Figure 1. (a) The eigenenergies as functions of the field(H). The dotted curves give those for $\Gamma = 0$, and the solid curves give eigenenergies for $\Gamma = 0.1$. (b) The time dependencies of the magnetization $M(t)$ for various values of the sweeping speeds $v = 0.005, 0.01, 0.02, 0.03, 0.05$ and 0.1. The bold solid curve denotes the adiabatic change.

First we study the one-dimensional transverse Ising model. In Fig. 2(a), we depict the eigenenergies as functions of H with $\Gamma = 0.5J$ ($N = 6$). In the case $H = 0$, a quantum phase transition takes place at $J = \Gamma$. Also at $H = 0$, the Hamiltonian is expressed in terms of fermion annihilation and creation operators, c_q and $c_q^\dagger$ as

$$\mathcal{H} = 2\sum_q \left[\sqrt{\Gamma^2 + 2\Gamma J\cos q + J^2}\, c_q^\dagger c_q + \text{const.}\right]. \tag{6}$$

Using this dispersion relation, we can calculate the energies of low energy states. In Fig. 2(b), we depict the size dependence of the energy gaps between the ground state and the excited states at $\Gamma = 0.5J$. We find that the energy gap between the ground state and the first excited state ΔE_{01} becomes exponentially small which represents the symmetry breaking phenomenon below the critical point ($\Gamma < J$). On the other hand, the energy gap between the ground state and the second and third excited states, ΔE_{02} and ΔE_{03}, respectively, stays almost constant. The time evolution of this magnetization under field sweep

$$M(t) = \langle\Psi(t)|\sum_i \sigma_i^z|\Psi(t)\rangle \tag{7}$$

reflects the energy structure. Here, $\Psi(t)$ is the wavefunction in the dynamical process. When we slowly sweep the magnetic field $H(t)$ the magnetization shows a stepwise magnetization process as a sequence of LZS transitions at the avoided level crossing points [9]. If we sweep fast, then the magnetization shows a size-independent shape, which we call "quantum spinodal decomposition" [10]. The process sweeping Γ at $H = 0$ can be studied exactly [11].

Although, in one dimension, the model has no ordered phase at finite temperature, in higher dimensions, the model has an order-disorder phase transition at a finite temperature for small values of Γ. At $\Gamma = 0$ the system is the usual Ising model. Therefore, we have a phase diagram schematically depicted in Fig. 3.

When we change parameters along the solid arrow ($\Gamma = 0$) quantum fluctuations are absent, and the thermal fluctuation induces the phase transition. On the other hand, when we change

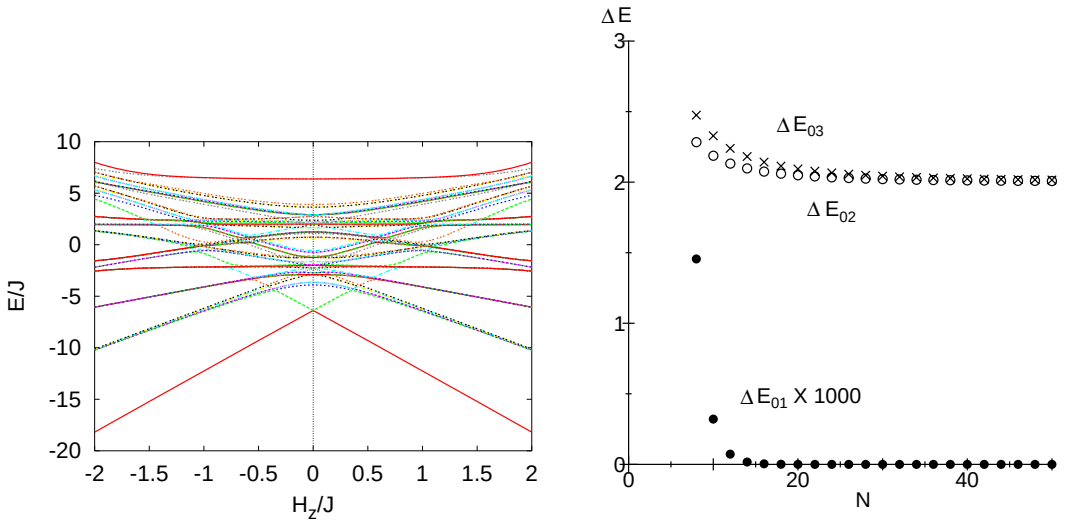

Figure 2. (a) Eigenenergies as functions of H of the one-dimensional transverse Ising model with $\Gamma = 0.5J$. (b) The energy gaps at $H = 0$ and $\Gamma = 0.5J$ between the ground state and the first excited state (dots), the second excited state (circles) and the third excited state (crosses).

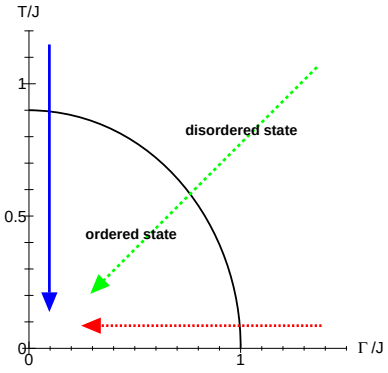

Figure 3. Schematic phase diagram of the transverse Ising model in high dimensions ($D \geq 2$).

parameters along the dotted arrow, ($T = 0$), the thermal fluctuations are absent, and the quantum fluctuation induces the phase transition.

3. Comparison of thermal and quantum fluctuations

First, let us compare the natures of the thermal and quantum fluctuations. In order to describe both fluctuations, it is convenient to express the state by the density matrix

$$\rho = \sum_{i=1}^{M} w_{ij} |i\rangle\langle j|. \tag{8}$$

In the classical case, the diagonal elements represent the probabilities of the state i, i.e. $P(i) = w_{ii}$. In the quantum system, the off-diagonal elements give the quantum fluctuations.

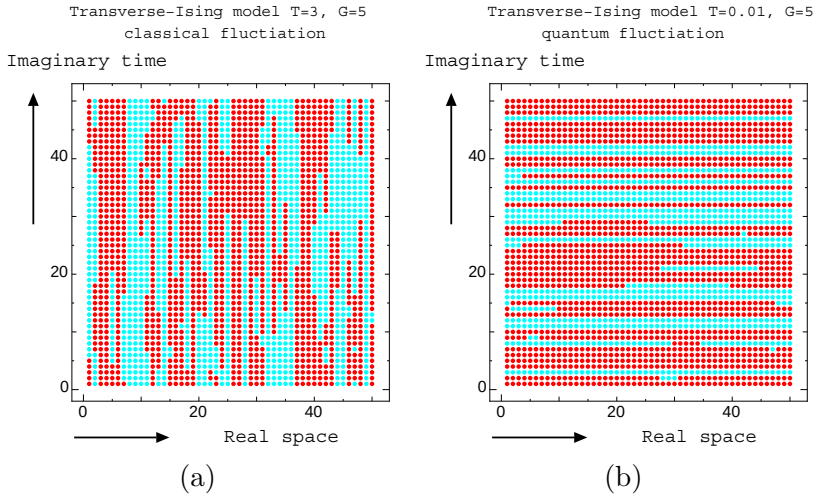

Figure 4. Typical configurations of (a) thermal ($T/\Gamma = 3/5$) and (b) quantum fluctuations ($T/\Gamma = 0.002$) in the quantum Monte Carlo simulation. The red points denote up spins, and the blue ones down spins.

The dynamics of the density matrix is given by the Bloch equation

$$i\hbar\frac{\partial}{\partial t}\rho = [\mathcal{H}, \rho]\,. \tag{9}$$

In order to find the density matrix for the equilibrium state, quantum Monte Carlo method can be used. Then, the density matrix is expressed by $(d+1)$-dimensional configuration using the Suzuki-Trotter decomposition which is a kind of path-integral representation of the density matrix [12]. The equilibrium density matrix of the model is expressed by

$$\rho = e^{-\beta\mathcal{H}}/Z, \quad Z = \mathrm{Tr}e^{-\beta\mathcal{H}}. \tag{10}$$

In order to study the nature of fluctuation, we study matrix elements of the density matrix which correspond to snapshots of quantum Monte Carlo simulation. A d-dimensional transverse Ising model is mapped into a $(d+1)$-dimensional Ising model $\{\sigma_i^k\}$ with anisotropic couplings

$$K_{\text{real space}} = \frac{\beta J}{M}, \quad \text{and} \quad K_{\text{imaginary time}} = -\frac{1}{2}\ln(\tanh\frac{\beta}{M}\Gamma). \tag{11}$$

If β/M is small, i.e. at a high temperature, $K_{\text{real space}}$ is small and $K_{\text{imaginary time}}$ is large. Thus, the fluctuation occurs in the real space. On the other hand, at low temperatures, the fluctuation occurs in imaginary axis. In Fig. 4, we depict typical configurations of (a) the thermal and (b) quantum fluctuations in the quantum Monte Carlo simulation.

3.1. Reentrant phenomena

In classical systems, we have pointed out that frustrated configurations cause non-monotonic developments of ordering. In some systems, the sign of the correlation function changes as a function of the temperature, i.e. an antiferromagnetic correlation appears at high temperatures while a ferromagnetic one at low temperatures. This kind of non-monotonic effect causes a reentrant phase transition where different types of phases appear successively when the temperature changes [13, 14]. There the distribution of density of states (entropy) takes an

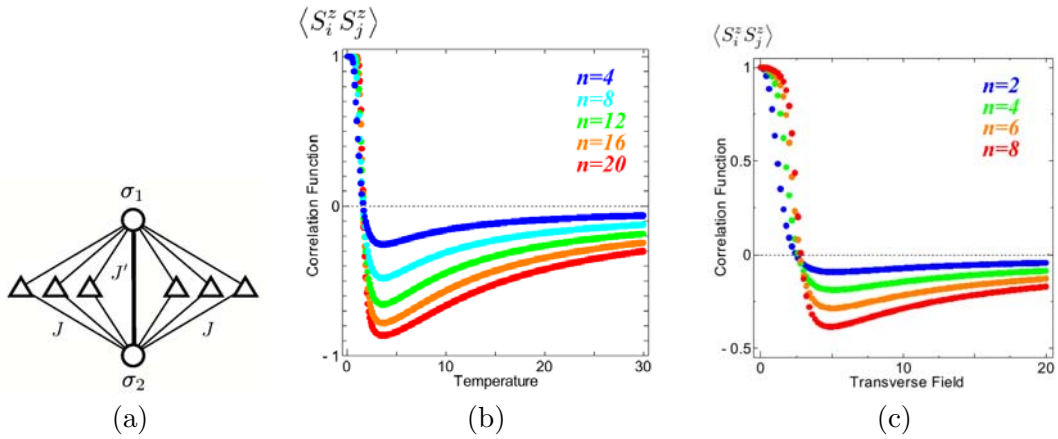

(a) (b) (c)

Figure 5. A typical example of reentrant type of the correlation function. (a) A frustrated lattice. The circles denote the spins σ_1 and σ_2, and the triangles denote the decoration spins s_k. (b) Correlation function between the spin 1 and 2 as a function of the temperature ($n = 4, 8, 12, 16$, and 20), and (c) correlation function between the spin 1 and 2 as a function of Γ. ($n = 2, 4, 6$ and 8).

important role. Similar behavior has been observed in the transverse Ising model with the change of Γ [15]. There, the quantum fluctuation is affected by the frustration as well as the thermal fluctuation. A typical example of reentrant type Γ dependence of the correlation function is depicted in Fig. 5 for a frustrated lattice whose Hamiltonian is given by

$$\mathcal{H}_{\text{reentrant}} = J'\sigma_1\sigma_2 - J\sum_{k=1}^{n}(\sigma_1 + \sigma_2)s_k, \quad \sigma_i = \pm 1, \quad \text{and} \quad s_i = \pm 1, \tag{12}$$

with $J = 1$ and $J' = \frac{n}{2}J$.

3.2. Quantum annealing

In order to find the ground state of a complicated system $\mathcal{H}_0$, there have been proposed various methods. The so-called annealing method is one of the typical methods for this purpose. In the usual thermal annealing method, the thermal fluctuations produce possible candidates of states for the update. Monte Carlo method provides an ensemble of states for an equilibrium state by making use of a kind of Markov chain (master equation). If we use only local updates of the state, the realization of equilibrium ensemble is often difficult due to the frozen effects due to energy barriers and/or entropy barriers [14]. To avoid the freezing, there have been introduced various techniques such as multi-canonical Monte Carlo method [16], temperature exchange Monte Carlo method [17], etc. These methods employ a wide variety of fluctuations that cause the sampling to be more efficient, and accelerate to converge to the desired ensemble. The Swendsen-Wang algorithm [18] introduces a graphical representation to realize an efficient sampling in which cluster flips performed systematically.

Quantum fluctuations have been also used to efficiently search for the ground state, a technique that is called quantum annealing [2]. There the transverse field generates the quantum fluctuations. In the limit $\Gamma = \infty$, the state is the ferromagnetic state aligned to the x direction, which is the sum of all state

$$|F_x\rangle = \sum_{\sigma_1=\pm 1,\cdots,\sigma_N=\pm 1} |\sigma_i, \cdots, \sigma_N\rangle \tag{13}$$

is the ground state. When we reduce Γ gradually, the ground state changes adiabatically to the ground state of the original system. Generally we believe that there is no level crossing during the process $\Gamma \to 0$. Thus when we gradually reduce Γ, the ground state moves to the ground state at $\Gamma = 0$. This is the idea of the quantum annealing and has been successfully applied to various systems. Recently, the proof of the convergence has been given [19] for the quantum case as well as the classical case [20].

Here let us consider mechanisms to find the ground state. In order to find ground state, the simplest method is the exact diagonalization. If the system has K states we need K^2 memory. In order to reduce the necessary memory several methods have been invented, e.g. the power method, Lanczos method, etc. Then we need the memory proportional to K. In the 1/2-spin system, $K = 2^N$. Thus, these methods correspond to a full search over all the states. On the other hand, the Monte Carlo method in the classical systems requires only memory of the order N. In the quantum Monte Carlo method, we need memory of the order $N \times N_\tau$, where N_τ is the number of points along the imaginary axis. Thus, both systems have advantage when N is large. As we saw in Fig. 3, beside the thermal annealing (the solid line) and the quantum annealing (the dotted line), there are many other paths to reach the ground state. It would be an interesting problem to find the optimal path starting from the point ($T = \Gamma = \infty$). The quantum annealing method could be applied to very wide variety of systems. For example, applications to an classification into clusters [21], and also to the variational Bayes inference [22] are being developed.

4. Other types of quantum fluctuation

The so-called single molecular magnets such as Mn_{12}, Fe_8, V_{15}, etc. have attracted interests because they show a sign of quantum dynamics through the discrete energy level structure. The degree of freedom inside the single molecules would be used as a storage of information. Above we have studied the quantum fluctuation in the transverse Ising model. In this section, we study other types of quantum fluctuations. In general, when an interaction $\mathcal{H}'$ does not commute with the order parameter M (the magnetization in the above case)

$$[M, \mathcal{H}'] \neq 0, \tag{14}$$

the magnetization is no longer good quantum number, and we say that the system has the quantum fluctuations. Then we find interesting properties in the dynamics of M under the change of parameters of the Hamiltonian. Here we introduce some of examples.

4.1. Dzyaloshinsky-Moriya interaction in the triangle lattice

As the important interaction which does not commute with the magnetization and causes a kind of quantum mixing is the Dzyaloshinsky-Moriya (DM) interaction

$$\mathcal{H}_{\rm DM} = \sum_{<ij>} \boldsymbol{D}_{ij} \cdot \boldsymbol{S}_i \times \boldsymbol{S}_j. \tag{15}$$

This interaction is characterized the vectors $\boldsymbol{D}_{ij}$ and thus the vectors must be compatible with the symmetry of the lattice. Here, we study the effect of this interaction on a system consisting of three spins making an equilateral triangle. The Hamiltonian is given by

$$\mathcal{H}_3 = J \sum_i^3 \boldsymbol{S}_i \cdot \boldsymbol{S}_{i+1} - \sum_i^3 \boldsymbol{D}_i \cdot \boldsymbol{S}_i \times \boldsymbol{S}_{i+1} - \boldsymbol{H} \sum_{i=1}^3 \boldsymbol{S}_i, \tag{16}$$

where $\boldsymbol{S}_4 = \boldsymbol{S}_1$. Because of the symmetry, it is required that $D_1^z = D_2^z = D_3^z$ and

$$\begin{pmatrix} D_1^x \\ D_1^y \end{pmatrix} = R \begin{pmatrix} D_2^x \\ D_2^y \end{pmatrix} = R^2 \begin{pmatrix} D_3^x \\ D_3^y \end{pmatrix}, \tag{17}$$

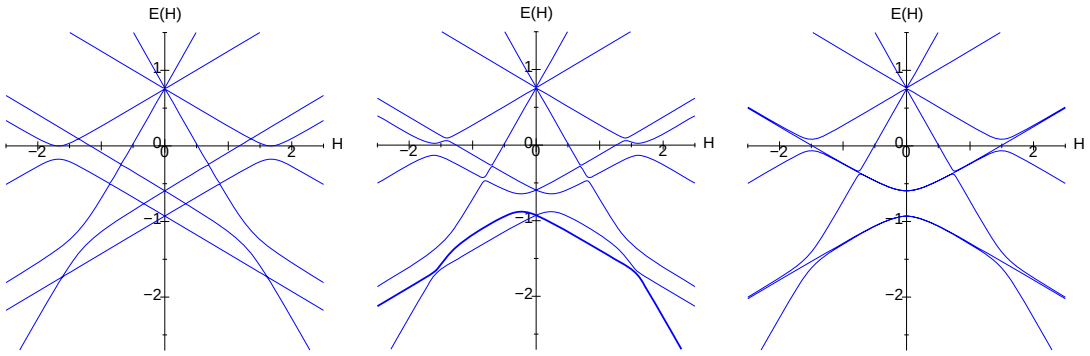

(a) (b) (c)

Figure 6. Energy structure of an equilateral triangle lattice with DM interaction ($D_x = D_z = 0.2J$) for (a) $\theta = 0°$, (b) $\theta = 45°$and (c) $\theta = 90°$, where $\boldsymbol{H} \cdot \boldsymbol{D} = \cos\theta$.

where R is a matrix of the rotation of 120°. Here it should be noted that when $\boldsymbol{H}$ is parallel to $\boldsymbol{D}$, the magnetization along the field commutes with the Hamiltonian and no adiabatic transition takes place (Fig. 6(a)). On the other hand, if they are not parallel, avoided level crossing structures appear. In Fig. 6, we show the energy structures as a function of the field for the case the angle between $\boldsymbol{H}$ and $\boldsymbol{D}$ is 0°, 45° and 90°. Avoided level crossing structures also appear at the crossing of the states with $M = 1/2$ and $M = 3/2$.

In Fig. 6(b), we have the following interesting characteristic of the adiabatic change of the magnetization. We start from the ground state in a large positive H where the magnetization is almost $+3/2$. When we reduce the magnetization from it, the state follows the curve drown by a thick curve, and it goes to a level with $M = -1/2$ at large negative H. If we start from the ground state in a large negative H, it goes to the state of $M = 1/2$. This indicates that the adiabatic change does not follow the ground state. The double degeneracy of the $S = 1/2$ states are characterized by the chirality, because the eigenstates of the states for the translation operation are $e^{i2\pi/3}$ and $e^{i4\pi/3}$. In the presence of the DM interaction the states with different chirality are not degenerate. The same property holds for other cases except the case of $\theta = 0°$ (e.g. Fig. 6(c)). Various interesting magnetization loops in a field cycling appear according to the structures of the adiabatic energy levels [24]. As we saw above, the DM interaction causes energy gaps which strongly depend on the direction of the field. In contrast, it is known that the hyperfine interaction between the electron spins and nuclear spins causes gaps which are independent of the field direction [25]. Recently, coherent quantum dynamics of driven Rabi oscillation was observed in V_{15} [26].

4.2. Particle conveyance by a trap potential

When we consider the motion of particles, the operators of the momentum $\boldsymbol{p}$ and the position $\boldsymbol{x}$ do not commute. Thus, in the process of acceleration of the particle, there occurs various interesting quantum effects [27].

4.3. Realization of the Nagaoka-ferromagnetism by removal of an electron

It is known that the total spin of the Hubbard model is zero in the half-filled bipartite lattices, while it takes the maximum value when an electron is removed. This mechanism is called "Nagaoka ferromagnetism" [28]. We can demonstrate an adiabatic change between these state if we add an extra lattice point and absorb an electron by a strong chemical potential in a

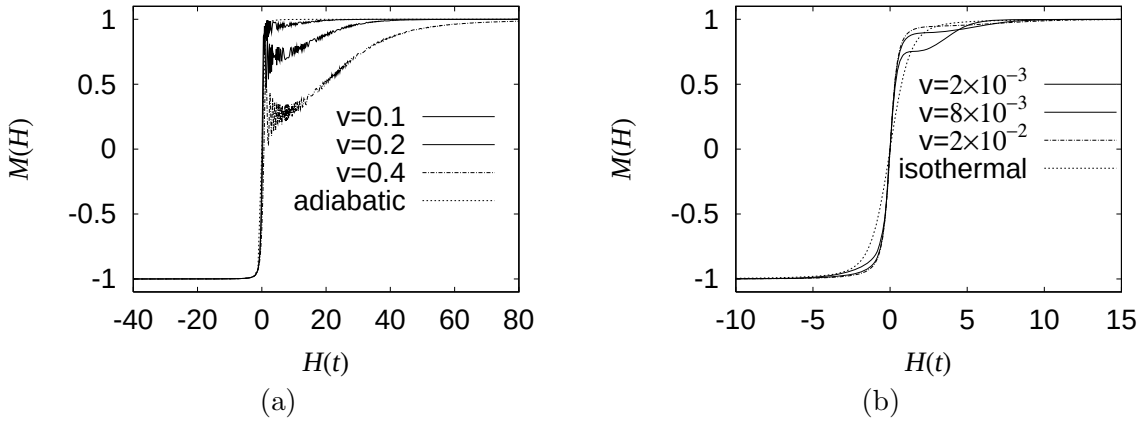

Figure 7. (a) Magnetization process for $v = 0.1, 0.2$, and $v = 0.4$. (b)Magnetization process for $v = 0.001, v = 0.006$, and $v = 0.01$. (From J. Phys. Soc. Jpn. **70** (2001) 3385.)

magnetic field [29].

5. Dissipation effect

Now, we discuss effects of environments on the adiabatic process, which we call 'magnetic Foehn effect' [30]. Here, we consider the effects in the simplest model (Eq. (1)) to simulate the phonon-bottleneck effect found in a magnetic molecule V_{15} which belongs to this category [5].

We use a quantum master equation [31, 32] for various sweeping velocities.

$$\frac{\partial \rho(t)}{\partial t} = -\frac{i}{\hbar}[\mathcal{H}, \rho(t)] - \lambda\left([X, R\rho(t)] + [X, R\rho(t)]^{\dagger}\right), \tag{18}$$

where X is a system operator through which the system couples with the bath, R is a bath operator, and λ is the coupling constant between the system and the reservoir. From now on, we set parameters as $\Gamma = 0.5, T = 1.0$, and $\lambda = 0.001$. In Fig. 7(a), we present the magnetization curves for fast sweeping rates, $v = 0.1, 0.2$, and 0.4. Here we clearly find that the magnetic plateau decreases when v increases, which is consistent with Eq. (4). The increase of the magnetization after the plateau is a process of relaxation to the equilibrium state caused by the dissipation term. The dotted line there denotes the adiabatic curve of the magnetization. In the case of much slow sweeping rates, we again find the magnetic plateau as shown in Fig. 7(b), although the LZS transition probability (Eq. (4)) is almost one in these sweeping rates. Here, the sweeping rates are $v = 2 \times 10^{-3}, 8 \times 10^{-3}$, and 2×10^{-2}. The dotted line denotes the isothermal curve of the magnetization at the present temperature. We should note that the magnetic plateau in this figure increases when v increases, which is opposite to the fast sweeping case.

The quantum master equation brings the density matrix to that of the equilibrium of the system [32]. However, contact with the thermal bath causes modification of the system, which has been known as the Lamb shift. It has been shown that this effect is systematically taken into account by modifying the master equation [33].

6. Summary and Discussion

Here we explored properties of quantum fluctuations and possible manipulations of them. Because the nature of quantum fluctuation is different from that of thermal fluctuation, it could play important roles in information processing. In particular, we expect that the nontrivial properties of quantum dynamics would provide new developments of information processing.

Acknowledgments
This work was partially supported by a Grant-in-Aid for Scientific Research on Priority Areas "Physics of new quantum phases in superclean materials" (Grant No. 17071011), and also by the Next Generation Super Computer Project, Nanoscience Program of MEXT. We also thank the supercomputer center, Institute for Solid State Physics, University of Tokyo for the use of the facilities.

References

[1] Nielsen M A and Chuang I L 2000 *Quantum Computation and Quantum Information* (Cambridge: Cambridge University Press)
[2] Kadowaki T and Nishimori H 1998 *Phys. Rev.* E **58** 5355; Das A and Chakrabarti B K 2005 *Quantum Annealing And Related Optimization Methods* (New York: Springer-Verlag); Santoro G E and Tosatti E 2006 *J. Phys. A: Math. Gen.* **39** R393; Das A and Chakrabarti B K 2008 *Rev. Mod. Phys.* **80** 1061
[3] Thomas L, Lionti F, Ballou R, Sessoli R, Gatteschi D and Barbara B 1996 *Nature* **383** 145; Friedman J R, Sarachik M P, Tejada J and Ziolo R 1996 *Phys. Rev. Lett* **76** 3830
[4] Sangregorio C Ohm T, Paulsen C, Sessoli R and Gatteschi D 1997 *Phys. Rev. Lett.* **78** 4645; Wernsdorfer W and Sessoli R 1999 *Science* **284** 233
[5] Chiorescu I, Wernsdorfer W, Müller A, Bögge H and Barbara B 2000 *Phys. Phys. Lett.* **84** 3454
[6] Zener C 1932 *Proc. R. Soc. London* Ser A**137** 697; Landau L 1932 *Phys. Z. Sowjetunion* **2** 46; Stückelberg E C G 1932 *Helv. Phys. Acta* **5** 3207
[7] Miyashita S 1995 *J. Phys. Soc. Jpn.* **64** 3207; Miyashita S 1996 *J. Phys. Soc. Jpn.* **65** 2734.
[8] Chakrabati B K, Dutta A and Sen P 1996 *Quantum Ising Phase Transitions in Transverse Ising Models* (Heiderlberg: Springer-Verlag)
[9] De Raedt H, Miyashita S, Saito K, Garcia-Pablos D and Garcia N 1997 *Phys. Rev.* B **56** 11761
[10] Miyashita S, De Raedt H and Barbara B *unpublished*
[11] Dziarmaga J 2005 *Phys. Rev. Lett.* **95** 245701
[12] Suzuki M 1976 *Prog. Theor. Phys.* **56** 1454
[13] Miyashita S 1983 *Prog. Theor. Phys.* **69** 714; Kitatani H, Miyashita S and Suzuki M 1986 *J. Phys. Soc. Jpn.* **55** 865; Miyashita S and Vincent E 2001 *Eur. Phys. J* B **22** 203
[14] Tanaka S and Miyashita S 2005 *Prog. Theor. Phys. Suppl.* **157** 34
[15] Tanaka S and Miyashita S *unpublished*
[16] Berg B A and Neuhaus T 1991 *Phys. Lett.* B **267** 249; Berg B A and Neuhaus T 1992 *Phys. Rev. Lett.* **68** 9
[17] Hukushima K and Nemoto K 1996 *J. Phys. Soc. Jpn.* **65** 1604
[18] Swendsen R H and Wang J S 1987 *Phys. Rev. Lett.* **58** 86; Wolff U 1989 *Phys. Rev. Lett.* **62** 361
[19] Morita S and Nishimori H 2006 *J. Phys. A: Math. Gen.* **39** 13903; Morita S and Nishimori H 2007 *J. Phys. Soc. Jpn.* **76** 064002
[20] Geman S and Geman D 1984 *IEEE Trans. Pattern Anal. Mach. Intell.* **6** 721
[21] Kurihara K, Tanaka S and Miyashita S *unpublished*
[22] Sato I, Kurihara K, Tanaka S, Nakagawa H and Miyashita S *unpublished*
[23] Miyashita S and Nagaosa N 2001 *Prog. Theor. Phys.* **106** 533; De Raedt H, Miyashita S, Michielsen K and Machida M 2004 *Phys. Rev.* B **70** 064401
[24] Choi K Y, Matsuda Y H, Nojiri H, Kortz U, Hussain F, Stowe A C, Ramsey C and Dalal N S 2006 *Phys. Rev. Lett.* **96** 107202
[25] Miyashita S, De Raedt H and Michielsen K 2003 *Prog. Theor. Phys.* **110** 889
[26] Bertaina S, Gambarelli S, Mitra T, Tsukerblet B, Müller A and Barbara B 2008 *Nature* **453** 203
[27] Miyashita S 2007 *J. Phys. Soc. Jpn.* **76** 104003
[28] Nagaoka Y 1966 *Phys. Rev.* **147** 392
[29] Miyashita S 2008 *Prog. Theor. Phys.* **120** 785
[30] Saito K and Miyashita S 2001 *J. Phys. Soc. Jpn.***70** 3385
[31] Weidlich W and Haake F 1965 *Z. Phys.* **185** 30; Kubo R, Toda M and Hashitsume N 1985 *Statistical Physics II* (New York: Springer-Verlag); Louisell W H 1973 *Quantum Statistical Properties of Radiation* (New York: Wiley)
[32] Saito K, Takesue S and Miyashita S 2000 *Phys. Rev.* E **61** 2397
[33] Mori T and Miyashita S 2008 Dynamics of the Density Matrix in Contact with a Thermal Bath and the Quantum Master Equation *to appear in J. Phys. Soc. Jpn.* **77** (*Preprint* arXiv:0810.0626)